RNA-binding protein DAZAP1 promotes gastric cancer metastasis by enhancing NOTCH1 and JAG1 mRNA stability

SIYANG PENG[1], YIDONG CHEN[1], JIEKE WU[1], XIAODONG HUANG[1], LINJIE HONG[2], YANCI XIE[1], YUTING LEI[1], XIANGYANG WEI[1], PING YANG[1], JIEMING ZHANG[1], QIONG YANG[3], GUANGNAN LIU[1], AIMIN LI[1], SIDE LIU[1], JIAYING LI[3], WEIYU DAI[4], YANFENG HU[5], JING WANG[6], JING XIONG[1] and JIDE WANG[1]

[1]Guangdong Provincial Key Laboratory of Gastroenterology, Department of Gastroenterology, Nanfang Hospital, Southern Medical University, Guangzhou, Guangdong 510515, P.R. China; [2]Department of Gastroenterology, The Second Affiliated Hospital of Fujian Medical University, Quanzhou, Fujian 362000, P.R. China; [3]Department of Gastroenterology, The Key Laboratory of Advanced Interdisciplinary Studies Center, The First Affiliated Hospital of Guangzhou Medical University, Guangzhou, Guangdong 510120, P.R. China; [4]Department of Gastroenterology and Hepatology, Guangdong Provincial People's Hospital Guangdong Academy of Medical Sciences, Southern Medical University, Guangzhou, Guangdong 510080, P.R. China; [5]Department of General Surgery, Nanfang Hospital, Southern Medical University, Guangzhou, Guangdong 510515, P.R. China; [6]Department of Pathology, The First Affiliated Hospital, Guangzhou Medical University, Guangzhou, Guangdong 510163, P.R. China

Received November 4, 2025; Accepted January 19, 2026

DOI: 10.3892/ijo.2026.5863

Abstract. DAZ-associated protein 1 (DAZAP1), an RNA-binding protein and modulator of alternative splicing, participates in tumorigenesis. However, the potential oncogenic function and mechanism of DAZAP1 in gastric cancer (GC) are unknown. Gene expression analysis, including mRNA and protein level assessment by reverse transcription-quantitative PCR and western blotting, respectively, immunofluorescence, immunohistochemistry, *in situ* hybridization assays, tissue microarray, RNA immunoprecipitation and sequencing and mRNA stability assay were performed, as well as colony formation, EdU, wound healing, migration and invasion assays of GC cells. DAZAP1 displayed a significant upregulation in GC cells and served as an oncogene, as demonstrated by its overexpression promoting colony formation, EdU incorporation, wound healing, migration and invasion, and its knockdown suppressing these malignant phenotypes. Additionally, DAZAP1 upregulation was positively correlated with tumor progression and poor survival in individuals with GC. Functionally, DAZAP overexpression promoted proliferation, epithelial-mesenchymal transition (EMT) and migration/invasion of GC cells. Mechanistically, DAZAP1 physically bound NOTCH1 or JAG1 mRNA to regulate its stability. In addition, overexpression of DAZAP1 facilitated NOTCH1- and/or JAG1-mediated migration via EMT in GC cells. Changes in NOTCH1 or JAG1 expression were positively correlated with DAZAP1 expression when DAZAP1 was silenced or enhanced in GC. Finally, DAZAP1 modulated the activation of the NOTCH/JAG1 signaling pathway. DAZAP1 expression facilitated migration/invasion and mediated the stabilization of NOTCH1 or JAG1 mRNA, suggesting they may participate in GC progression.

Correspondence to: Professor Jide Wang or Professor Jing Xiong, Guangdong Provincial Key Laboratory of Gastroenterology, Department of Gastroenterology, Nanfang Hospital, Southern Medical University, 1023 South Shatai Road, Baiyun, Guangzhou, Guangdong 510515, P.R. China
E-mail: jidewang55@163.com
E-mail: xhsky0717@126.com

Key words: DAZ-associated protein 1, NOTCH1, JAG1, gastric cancer, metastasis, EMT

Introduction

Gastric cancer (GC) is the fifth leading main cause of cancer-associated morbidity and mortality worldwide, accounting for 5.6% of all new cancer cases (1,089,103 cases) and 7.7% of all cancer deaths (768,793 deaths) globally in 2020 (1). Although emerging therapies such as immunotherapy (2) and targeted therapy (3) have been developed, the prognosis remains poor due to late-stage diagnosis, limiting treatment efficacy. Globally, ~50% of GC patients are diagnosed at advanced (unresectable or metastatic) stages as of 2020, with an overall 5-year survival rate of only around 20% for all stages combined (1). Thus, elucidating the molecular mechanisms underlying GC initiation and progression is key.

RNA-binding proteins (RBP) are key regulators of gene expression through their roles in RNA metabolism (4,5). Most RBPs interact with mRNA and pre-mRNA, participating in splicing, stabilization and transport (5,6). Dysregulated RBP expression is implicated in numerous human diseases (6,7). For example, poly(A) binding protein cytoplasmic 1 (PABPC1) stabilizes p21-activated kinase 1

mRNA, promoting epithelial-mesenchymal transition (EMT) and GC migration/invasion (7). DAZ-associated protein 1 (DAZAP1), a part of the heterogeneous nuclear ribonucleoprotein (hnRNP) family, is an RBP (8,9). Abnormal expression of DAZAP1 regulates cancer cells (8,10). For example, DAZAP1 is significantly upregulated in oral squamous cell carcinoma (OSCC), promoting cell migration, invasion and the EMT process (10). It regulates post-transcriptional gene expression by binding target mRNAs via the 'UAGKWWR' motif (9,11,12). For example, DAZAP1 enhances hepatocellular carcinoma progression and modulates ferroptosis through interaction with SLC7A11 mRNA (12) and facilitates alternative splicing of kit ligand (KITLG) to trigger numerous myeloma cell proliferation (13). However, its role in regulating mRNA expression in GC remains poorly understood.

Notch is a canonical signaling pathway that comprises four Notch receptors (Notch 1, 2, 3 and 4) and five Notch ligands [Δ-like 1, 3 and 4 and Jagged (JAG)1 and 2] in mammals (14,15). NOTCH1 is most commonly found in cancer tissue (15,16). For example, elevated expression of NOTCH1 is associated with tumor invasion and lymph node metastasis of GC (16). Moreover, RBP insulin-like growth factor 2 mRNA-binding protein 2 directly binds T cell acute lymphoblastic leukemia oncogene NOTCH1 mRNA (17). JAG1 is highly expressed in GC and colorectal and breast cancer (18-21). JAG1 promotes cell migration/invasion and is associated with poor prognosis in breast cancer (20). Furthermore, RBP zinc finger protein 36 (ZFP36) directly binds JAG1 mRNA and is involved in mRNA decay (21). In addition, the Notch/JAG pathway is key in EMT during embryonic development, fibrotic disorder and cancer metastasis (22,23). Activation of Notch signaling induces EMT in tumor cells and JAG1-mediated Notch signaling triggers the EMT process, migration and invasion of malignant cells; these effects are abrogated by Notch silencing (23). To the best of our knowledge, however, the mechanism by which DAZAP1 post-transcriptionally regulates NOTCH1 or JAG1 expression to affect GC progression has not been examined.

The present study aimed to explore DAZAP1 expression in GC, elucidate its regulatory role in GC cell behavior and EMT progression, verify its effect on the mRNA stability of NOTCH1 and JAG1 and define the role of the DAZAP1-NOTCH1/JAG1 axis in GC development and its potential as a therapeutic target.

Materials and methods

Cell culture. Normal human gastric mucosal GES-1 and GC cell lines (HGC-27, MKN-74, SNU-216, MKN-45, AGS and SNU-719) were obtained from American Type Culture Collection and cultured in RPMI-1640 medium enriched with 10% FBS (both purchased from Gibco (Thermo Fisher Scientific). All cells were cultivated in a 37˚C incubator with 5% CO_2.

Data acquisition and bioinformatics analysis. The microarray or RNA sequencing datasets GSE70880 (ncbi.nlm.nih.gov/geo/query/acc.cgi?acc=GSE70880), GSE99416 (ncbi.nlm.nih.gov/geo/query/acc.cgi?acc=GSE99416) and GSE109476 (ncbi.nlm.nih.gov/geo/query/acc.cgi?acc=GSE109476) were downloaded from the Gene Expression Omnibus (GEO) database and analysis was conducted to obtain the differentially expressed genes (DEGs) between GC and healthy tissue samples, with the screening criterion set as a fold change >1.2. DEGs were integrated with RNA-binding protein (RBP) prediction data downloaded online from the RBPmap website (rbpmap.technion.ac.il/) (24). Bioinformatics analysis, including the construction of Venn diagrams, was performed using R software (v4.0.2; r-project.org/). The present study used expression levels of DAZAP1 from the FireBrowse (firebrowse.org/) and UALCAN (ualcan.path.uab.edu/) databases to further validate the results obtained from bioinformatics analysis. Gene searches were performed using the PubMed database (pubmed.ncbi.nlm.nih.gov/). To obtain EMT-related genes, the gene set from the EMT database (emtome.org) (25). The Cancer Genome Atlas (cancer.gov/tcga) database was used for bioinformatics analysis, focusing on the STAD (stomach adenocarcinoma) cohort. Kyoto Encyclopedia of Genes and Genomes (KEGG) pathway enrichment analysis for target genes was conducted with the WebGestalt database (webgestalt.org/). Analysis of potential transcription factors of DAZAP1 was performed using the AnimalTFDB v4.0 database (guolab.wchscu.cn/AnimalTFDB4/#/).

Tissue samples. Gastric adenocarcinoma tissue microarray (TMA; cat. no. HStm-Ade180Sur-04) was acquired from Shanghai Outdo Biotech Co Ltd. The TMA analysis included 90 GC samples and 90 matched adjacent healthy tissue samples (70 male; 20 female; median age, 65 years; age range, 34-83 years; distance, 5 cm). The use of tissue chips was approved by the Ethics Committee of Shanghai Outdo Biotech Co. Ltd. (approval no. SHYJS-CP-1804015).

A total of 10 formalin-fixed and paraffin-embedded GC specimens and adjacent healthy tissue specimens were collected from patients (seven male; three female; median age, 63 years; age range, 42-81 years) with GC at Nanfang Hospital (Guangzhou, China) between December 2023 and January 2024. Normal tissues were collected 5 cm from the tumor edge and immediately stored in liquid nitrogen at -196˚C for subsequent experimentation. The diagnosis of primary GC was validated by two pathologists. Patients who had received chemotherapy, radiotherapy or molecular-targeted therapy before surgery were excluded. These tissues were used for western blotting, reverse transcription-quantitative (RT-q) PCR and RNA *in situ* hybridization (ISH). The study received ethical approval from Nanfang Hospital, Southern Medical University (approval no. NFEC-202105-K18; Nanfang, China). All patients provided written informed consent.

Immunohistochemistry (IHC) and TMA analysis. A total of 10 paired GC tumor and adjacent non-cancerous gastric mucosa samples were surgically obtained in 2020 from the Department of Surgery, Nanfang Hospital, Southern Medical University, for analysis by IHC and western blotting. Table SI presents the antibodies used. All experimental protocols received approval from the Ethics Committee of Southern Medical University, China.

Following 24 h fixation with 4% paraformaldehyde at room temperature, tumor specimens were embedded in paraffin wax. Sections of 4-mm thickness were cut from paraffin-embedded tissue blocks and placed on glass slides. The slides were

deparaffinized using xylene, rehydrated using ethanol. For antigen retrieval, sections were microwaved in 0.01 mol/l sodium citrate buffer (pH=6.0) at 95˚C for 15 min. After immersing the sections in 3% hydrogen peroxide for 10 min at room temperature to inhibit endogenous peroxidase activity. Blocking was performed at room temperature for 20 min using 5% BSA; cat. no. A8850, Solarbio Science & Technology Co., Ltd.) to eliminate non-specific binding. The sections were then incubated overnight at 4˚C with the primary antibody against DAZAP1(Santa Cruz Biotechnology Co., Ltd.). Subsequently, they were incubated with the biotin-linked anti-Mouse IgG (cat. no. ab6823, dilution 1:1,000; Abcam) at room temperature for 30 min. Following another three PBS washes, chromogen detection was performed using DAB. The staining results were observed under a light microscope and analyzed using Image J 1.8 software (National Institutes of Health). Normal rabbit or mouse IgG (Sigma-Aldrich; Merck KGaA) was used as the isotype controls. The TMA was stained for DAZAP1 (Santa Cruz Biotechnology Co., Ltd.) according to the same protocol.

DAZAP1 staining intensity in carcinoma cells was scored as follows: 0 (negative), 1 (weak), 2 (moderate), and 3 (intense). Cells with scores of 0-1 were classified as low expression, while scores of 2-3 indicated high expression. The final IHC score for each sample was the average of evaluations by two independent observers.

Western blotting. Total protein from tissue or cells was extracted via RIPA lysis buffer (Beijing Solarbio Science & Technology Co., Ltd.) containing a protease inhibitor (MedChemExpress). The protein concentration of lysates was measured using the BCA assay. A total of 20 μg total protein were separated by 10% SDS-PAGE and were transferred to PVDF membranes. The membranes were treated with 5% non-fat dry milk at room temperature for 30 min. The membranes were blotted with primary antibodies (Table SI) overnight at 4˚C, followed by incubation with HRP-conjugated secondary anti-rabbit or anti-mouse antibodies (Abcam; cat. nos. ab7090 and ab97046; 1:6,000) for 1 h at room temperature. We confirm that β-tubulin (cat. no. 10094-1-AP, 1:5,000; Proteintech) was used as the reference protein . Enhanced chemiluminescence was utilized for visualization with the Pierce ECL Western Blotting Substrate (Thermo Fisher Scientific, Waltham, MA, USA), and densitometric analysis was performed using Image J 1.8 (National Institutes of Health, Bethesda, MD, USA).

Plasmid construct, transfection, lentiviral production and infection. DAZAP1-pEnter, DAZAP1-flag, DAZAP1-RNA recognition motif 1 (RRM1)-flag, DAZAP1-RRM2-flag, DAZAP1-C-terminal domain (CTD)-flag, NOTCH1-pEnter and JAG1-pEnter plasmids were constructed by Kidan Biosciences. Human DAZAP1 small interfering RNA (siRNA), including siRNA1, siRNA2 and siRNA pool (siRNAp; a 1:1 mixture of siRNA1 and siRNA2 with the total siRNA amount constant in the transfection system). NOTCH1-siRNAp, JAG1-siRNAp and scrambled siRNA non-specific control (Scr-siRNA) were synthesized by Shanghai GenePharma Co., Ltd. DAZAP1, NOTCH1 and Scramble shRNA were all purchased from GenePharma Co., Ltd. Both short hairpin (sh)RNAs and siRNAs were used. The siRNAs were applied for short-term functional assays, while shRNAs were used to establish stable cell lines and xenograft assays. Briefly, cells were plated in 6-well culture plates at a density of $3x10^5$ cells per well. At 30-50% confluency, the cells were transfected with 50 nM target siRNA or Scr-siRNA via Lipo8000 (Beyotime Institute of Biotechnology) transfection reagent, at 37˚C for 6 h. Subsequent experiments were conducted on the cells at 48 h post-transfection, and the transfection efficiency was validated by RT-qPCR) and western blot assays.

To establish stable AGS cell lines, the cells were transduced with lentiviruses for target gene manipulation (2nd-generation lentiviral system) purchased from GeneChem, Inc. The lentiviral vectors were engineered to express green fluorescent protein (GFP) as a reporter gene; with overexpression and knockdown constructed via GV348 and GV493 vectors (1 μg/μl, GenePharma, Inc). Lentiviral particles were produced by co-transfecting 293T cells (ATCC, USA) with 8 μg lentiviral target plasmid, 4 μg packaging and 2 μg envelope plasmid at 37˚C for 6 h; viral supernatants were collected at 48-72 h post-transfection. AGS cells were seeded at $5x10^5$ cells/well in 6-well plates and cultured to 80% confluency, then transduced with the lentivirus at MOI=100 with polybrene and transfection reagent A (GenePharma, Inc.) at 37˚C for 24-48 h following the manufacturer's protocol. Puromycin (10 μg/ml) was added at 72 h post-transduction for stable cell selection over 7 days; stably infected cells were maintained in 10 μg/ml puromycin and subjected to subsequent experiments 2-3 days after the completion of selection. Table SII lists the siRNA and shRNA target sequences.

RT-qPCR. Total RNA was isolated from AGS and MKN-45 cells, as well as 10 pairs of human GC and their adjacent normal tissues. The extraction was performed using TRIGene Plus reagent (cat. no. ZP108-101S, Genestar) in accordance with the manufacturer's instructions. RT was performed in strict accordance with the manufacturer's instructions for the was conducted via Hieff® Fast Cell SYBR Green RT-qPCR Kit (cat. no. 11172ES40, Shanghai Yeasen Biotechnology Co., Ltd.). RT-qPCR was conducted via SYBR Green Master Mix (Shanghai Yeasen Biotechnology Co., Ltd.) according to the manufacturer's guidelines. The thermocycling conditions were as follows: Initial denaturation at 95˚C for 2 min, followed by 40 cycles of denaturation at 95˚C for 15 sec and combined annealing/extension at 60˚C for 30 sec (two-step PCR). Quantification of relative levels of genes was conducted via the $2^{-\Delta\Delta Cq}$ method (26), and then normalization to the internal reference gene GAPDH was conducted. Table SIII illustrates the primer sequences.

Colony-forming assay. A total of 1,000 transfected cells were plated into 12-well plates and cultivated in a 37˚C, 5% CO_2 incubator for 10-12 days. All liquids were removed, 4% paraformaldehyde was used to fix them for 30 min at room temperature, then crystal violet was used for staining at room temperature for 15 min. Colonies were defined as cell populations large enough to be observed with the naked eye and were counted manually directly under a Zeiss microscope.

EdU assay. MKN-45, AGS and MKN-74 cells were cultured in 10 μM EdU-supplemented medium (Guangzhou RiboBio Co., Ltd.; cat. no. #C10310) for 4 h at 37˚C. Following removal of the EdU-supplemented medium, 4% paraformaldehyde was used to fix the cells at room temperature for 60 min. After washing with PBS solution and subsequent incubation with Apollo and Hoechst 33258 dyes at 37˚C, images were obtained via a fluorescence microscope. Proportion of EdU-positive staining was calculated as follows: EdU-stained cells/Hoechst-stained cells) x100%.

Wound healing assay. Serum starved MKN-45, AGS and MKN-74 cells were seeded into a 6-well culture plate at a density of $5x10^5$ cells/well and grown to 100% confluence. After cells were rinsed with PBS, they were scratched. Images were captured under an inverted light microscope. For MKN-45 cells, imaging was performed at 0, 24 and 48 h. For AGS and MKN-74 cells, imaging was conducted from 0 to 24 h at 12 h intervals. Migration index was calculated as follows: (Original wound width-wound width after healing)/ original wound width x100%.

Migration and invasion assay. Migration assays were performed via Transwell chambers in 24-well plates (BD Biosciences; cat. no. #353092). MKN-45 ($8x10^4$), AGS ($2x10^4$ cells) or MKN-74 cells ($2x10^4$ cells) were suspended in 100 μl serum-free RPMI 1640 medium (Gibco, Thermo Fisher Scientific) and plated in the top chambers, while the bottom chambers contained 700 μl RPMI-1640 medium with 20% FBS. After incubating for 48 h at 37˚C , non-migrated cells on the top membrane surface were removed with a cotton swab. Then, 4% paraformaldehyde was utilized to fix the migrated cells on the bottom surface for 60 min at room temperature, 0.1% crystal violet was used to stain them for 60 min at 37˚C and counting was conducted in four randomly selected high-power fields of view/sample under a light microscope (Zeiss microscope). For invasion assays, the top chambers were coated with Matrigel (cat. no. #358248, Corning, Inc.) at 37˚C for 30 min to allow for solidification; all other procedures were identical to the migration assay.

F-actin cytoskeleton staining. MKN-45 ($1x10^4$ cells) were cultured in a 24-well plate overnight at 37˚C. Cells were fixed with 4% paraformaldehyde at room temperature for 15 min, permeabilized with 0.1% Triton X-100 at room temperature for 10 min, and blocked with 5% FBS at room temperature for 30 min. F-actin staining was performed with rhodamine-conjugated phallotoxin (5 U/ml, Molecular Probes; Thermo Fisher Scientific, Inc.) according to the manufacturer's guidelines. Nuclei were stained with Hoechst33258 at room temperature for 10 min in the dark. F-actin cytoskeleton staining was assessed using a fluorescence microscope.

Immunofluorescence staining. Following washing in PBS, 4% paraformaldehyde was used to fix the MKN-45 cells for 15 min at room temperature. Following permeabilization with PBS containing 0.2% Triton X-100 for 5 min, cells were blocked with 10% goat serum (cat. no. ZLI-9056, Beijing Zhongshan Jinqiao Biotechnology Co., Ltd.) at 37˚C for 30 min. Cells were incubated with primary antibodies against E-cadherin (1:200, Proteintech Group, Inc.) and Vimentin (1:200, Cell Signaling Technology, Inc.) at 4˚C overnight. After three rinses with PBS, the cells were incubated with fluorochrome-conjugated secondary antibodies (1:100, cat. no. ZF-0512/ZF-0513, Beijing Zhongshan Jinqiao Biotechnology Co., Ltd., Alexa Fluor® 488/Alexa Fluor® 594 Conjugate) at 37˚C for 1 h in the dark. Nuclear counterstaining was performed with Hoechst 33258 dye at room temperature for 10 min in the dark, followed by two washes with PBS to remove excess dye. The stained cells were observed under a fluorescence microscope and all fluorescent images were acquired and analyzed using Image J 1.8 (National Institutes of Health, Bethesda, MD, USA).

RNA immunoprecipitation (RIP). Magna RIP RBPs Immunoprecipitation kit (MilliporeSigma) was used according to the manufacturer's instructions. In brief, cells were subjected to centrifugation at 300 x g for 5 min at 4˚C, the cells were suspended in 200 μl RIP lysis buffer (MilliporeSigma) provided in the kit that contained 1 μl protease inhibitor cocktail and 0.5 μl RNase inhibitor. A total of 200 μl lysate was used per IP reaction. A total of 5 μg anti-mouse DAZAP1 and mouse IgG isotype control antibody (MilliporeSigma) were added to the magnetic bead suspension, and the mixtures were gently shaken at room temperature for 1 h to form bead-antibody complexes. The bead-antibody complexes were allowed to sit at 4˚C overnight. Magnetic bead-RNA-protein complexes were washed three times with the RIP wash buffer 1 and 2 provided in the kit using a magnetic stand for magnetic separation of the complexes. After the RNA-protein complexes coupled to the beads were isolated, total RNA was extracted from the isolated complexes and subjected to sequencing analysis for target gene detection.

RIP sequencing (RIP-seq). Anti-DAZAP1 antibody was utilized to immunoprecipitate DAZAP1-RNA complexes, with input as the control (IgG). DAZAP1-bound RNAs were extracted via TRIzol, and a cDNA library was created via the TruSeq RNA library preparation kit (Illumina, Inc. cat. no. RS-122-2201), the quality and integrity of the processed RNA samples were verified using a Agilent 2100 Bioanalyzer (Agilent Technologies) prior to library construction. Sequencing was performed on the Illumina HiSeq X Ten platform by ABLife Inc. with 150 bp paired-end sequencing; the sequencing reaction was conducted using the HiSeq X Ten Reagent kit v2.5 (300 cycles; cat. no. FC-510-1003; Illumina, Inc.). The final library was loaded at a concentration of 10 pM, and the molar concentration was measured via Qubit 4 Fluorometer with Qubit dsDNA HS Assay kit (Thermo Fisher Scientific, Inc.; cat. no. Q32854). Raw sequencing data were analyzed using HISAT2 (v2.2.1; daehwankimlab.github.io/hisat2/), StringTie (v2.2.1; ccb.jhu.edu/software/stringtie/) and DESeq2 (v1.38.3; bioconductor.org/packages/release/bioc/html/DESeq2.html) for read alignment, transcript assembly and differential expression analysis, respectively.

mRNA stability assay. Scr-siRNA, DAZAP1-siRNAp, DAZAP1-siRNA1 and DAZAP1-siRNA2 were transfected into cells. After 24 h at 37˚C, the medium was substituted with medium (Gibco; Thermo Fisher Scientific; cat. no. 11875093). enriched with actinomycin D (10 μg/ml, MedChemExpress)

or DMSO. Total RNA was collected at 0, 2, 4, 6 and 8 h post-actinomycin D treatment using TRIGene Plus reagent (cat. no. ZP108-101S, Genestar) and mRNA half-life was estimated by determining NOTCH1 and JAG1 mRNA levels at each time point via RT-qPCR (normalized to GAPDH RNA) and curve fitting with the one-phase decay model in GraphPad Prism 9 (Dotmatics). NOTCH1 or JAG1 mRNA relative levels were assessed by RT-qPCR as aforementioned. mRNA levels were normalized to those of GAPDH RNA.

RNA in situ hybridization (ISH). ISH was conducted to observe NOTCH1 or JAG1 expression in GC specimens with locked nucleic acid-based ISH via digoxigenin-labeled miRCURY miRNA probes (Exiqon; Qiagen GmbH). DNA probes designed for the spatial expression analysis of mRNA were derived from the cDNA plasmid pGEM-T Easy (Promega, cat. no. A1360). Both probes had a length of 36 nucleotides, and the specific sequences of the probes used for ISH are illustrated in Table SIV. GC tissue was fixed with 4% paraformaldehyde at 4˚C for 24 h, embedded in paraffin and cut into 4 μm-thick serial sections on poly-L-lysine-coated glass slides (Thermo Fisher Scientific; cat. no. 12-550-15). The slides were deparaffinized, rehydrated and incubated with Proteinase K (Roche Diagnostics; cat. no. 3115887001) at 37˚C for 15 min, slides were then subjected to post-fixation with 4% paraformaldehyde at room temperature for 10 min and followed by washing with PBS. Pre-hybridization was performed with 5X saline-sodium citrate buffer (SSC; Sigma-Aldrich; cat. no. S6639) hybridization buffer (without probe) at room temperature for 15 min, followed by probe denaturation at 95˚C for 1 min. NOTCH1 mRNA and JAG1 mRNA probes (final concentration, 50 nM) were applied for hybridization in 5X SSC hybridization buffer with probe at 50˚C for 1 h. The slides were rinsed with 2.0 and 0.1X SSC (at 50˚C for 15 min each (30 min total) to remove excess probes, then blocked with 10% goat serum (Thermo Fisher Scientific; cat. no. 16210064) at RT for 30 min . An overnight incubation was performed with an anti-digoxigenin alkaline phosphatase-conjugated primary antibody [1:1,000, Roche Diagnostics (Shanghai) Co,. Ltd.; cat. no. 11093274910] at 4˚C.BCIP/NBT Chromogenic Detection System (Roche Diagnostics; cat. no. 11681451001) was used to visualize the hybridization signals. Nuclear fast red (Sigma-Aldrich; cat. no. N3020) was used to counterstain the slides at room temperature for 1 min, and mounting was performed via an aqueous solution. For each patient, four slides were hybridized with the NOTCH1 mRNA or JAG1 mRNA probe. Hybridization signals were observed under a light microscope and ImageJ v1.8 (National Institutes of Health) was used for signal intensity analysis.

Xenograft assay. A total of 24 nude female BALB/c mice (nu/nu; age, 4-6 weeks; weight, 20-22 g) were obtained from the Guangdong Medical Laboratory Animal Center (Guangzhou, China) and housed in specific-pathogen-free conditions were as follows: Temperature, 20-26˚C; humidity, 50-70%; light/dark cycle, 12/12-h; free access to food/water. The Animal Ethics Committee of Southern Medical University and Nanfang Hospital approved the animal experiments (approval no. IACUC-LAC-20250111-002).

For the tail vein-lung metastasis model, two groups of mice were utilized to assess the metastatic capability of malignant cells. The first group comprised the shRNA and DAZAP1-shRNA groups, while the second group included Vector + Scr-shRNA, DAZAP1 + Scr-shRNA, Vector + NOTCH1-shRNA, DAZAP1 + NOTCH1-shRNA, DAZAP1 + NOTCH1-shRNA + Vector and DAZAP1 + NOTCH1-shRNA + JAG1. An injection of $5x10^6$ lentivirus (LV)-transfected cells was administered into the tail veins of nude mice, which were euthanized after 30 days via CO_2 asphyxiation using a gradual-fill approach, with the gas introduced at a rate of 30% of the chamber volume/min. Cervical dislocation was performed to confirm death. Death was confirmed by disappearance of pain response, no reaction when the toes were pressed with hands or tweezers and cessation of heartbeat and respiration. The humane endpoint was body weight loss >20%; no animals met this endpoint during the experimental period. Subsequently, the lung metastases were counted. Paraffin-embedded lung tissues were sectioned into 4 μm sections and stained with hematoxylin and eosin and vimentin antibody as aforementioned.

Statistical analysis. Statistical analyses were performed using SPSS version 25.0 (IBM Corp.) and GraphPad Prism 10.1.2 (Dotmatics). All experiments were conducted in triplicate. All data are presented as the mean ± SD. For normally distributed continuous variables, Student's t-test (paired) or one-way ANOVA with Dunnett's post hoc test was applied as appropriate. For non-parametric comparisons, the Mann-Whitney U test was used. The Pearson correlation coefficient was used to assess the correlation between variables. Kaplan-Meier survival analysis was performed to evaluate overall or progression-free survival and the log-rank test was used to compare survival differences between groups. A two-tailed P-value <0.05 was considered to indicate a statistically significant difference.

Results

DAZAP1 is upregulated in GC. To identify novel protein coding genes involved in the onset and progression of GC, the present study assessed the microarray data of GSE70880, GSE99416 and GSE109476 downloaded from the GEO database and visualized the DEGs in GC and normal tissue samples (Fig. 1A). A total of 19 genes were up- and 17 were downregulated in the GSE109476 dataset, 81 genes were up- and 30 downregulated in the GSE70880 dataset and 48 genes were up- and 37 downregulated in the GSE99416 dataset. The intersection of the datasets demonstrated that only DAZAP1 was upregulated, and three genes (PPARGC1A, CIRBP, PABPC4) were downregulated. DAZAP1 was selected for further study due to its enhanced potential for use as an early diagnostic marker or intervention target (8-12). DAZAP1 was highly expressed in most tumors compared with adjacent healthy tissues based on FireBrowse and UALCAN databases (Fig. S1A and B). Expression of DAZAP1 was increased in GC compared with normal samples (Fig. 1B). Compared with normal gastric cell line GES-1, DAZAP1 protein expression was markedly upregulated in HGC-27, MKN-74, SNU-216, MKN-45, AGS and SNU-719 cells (Fig. 1C). IHC was performed to determine the intensity of the DAZAP1 staining (Fig. 1D). TMA showed

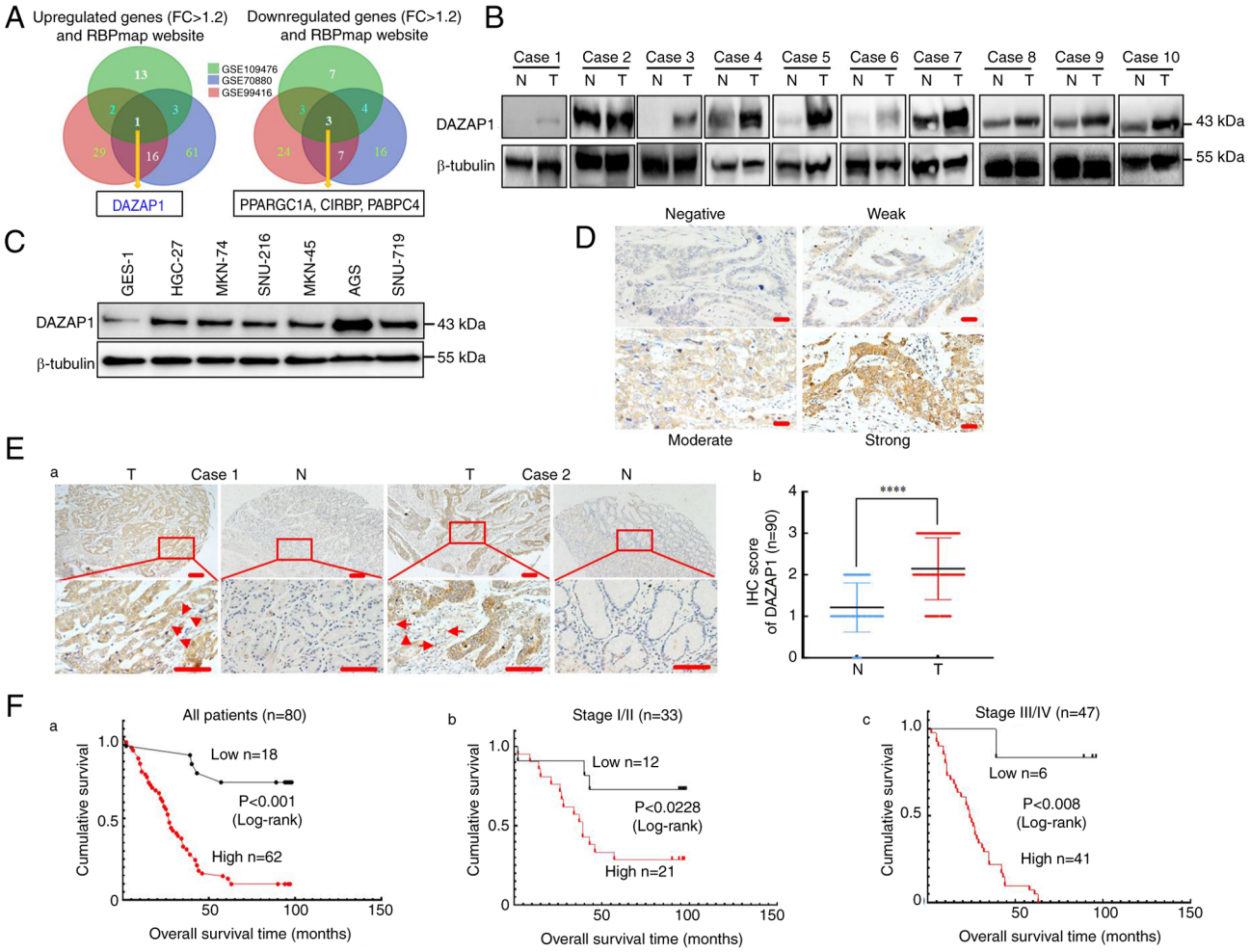

Figure 1. DAZAP1 is upregulated in GC. (A) Differentially expressed genes in the three Gene Expression Omnibus datasets and the RBPmap website. (B) Relative expression of DAZAP1 in 10 GC and their adjacent N tissues was examined by western blot assay. β-tubulin was used as the internal control. (C) Expression of DAZAP1 protein in six human GC and normal mucous cell line GES-1. (D) Representative staining of DAZAP1 intensity using IHC. (Ea) Representative gastric tissue from two cancerous and non-cancerous patients. Expression of DAZAP1 in normal and malignant human gastric tissue was detected by tissue microarray. The arrows indicate the cells with epithelial-to-mesenchymal transition) morphological alterations. (Eb) Expression of DAZAP1 was determined in N and T gastric tissue. Scale bar, 100 μm. Kaplan-Meier survival analysis of overall survival in (Fa) all patients and those with (Fb) early and (Fc) late stage GC (according to DAZAP1 expression. The log-rank test was used to calculate P-values. ****P<0.001. DAZAP, deleted in azoospermia-associated protein 1; GC, gastric cancer; N, normal tissue; T, tumor tissue; PPARGC1A, peroxisome proliferator-activated receptor gamma coactivator 1 alpha; CIRBP, cold inducible RNA-binding protein; PABPC4, poly(A)-binding protein cytoplasmic; FC, fold-change; IHC, immunohistochemistry.

upregulation of DAZAP1 in tumor tissue (Fig. 1Ea). DAZAP1 deposition was displayed in the stroma, with scattered malignant cells in the peripheral margin of the tumors (tumor-associated stromal cells), and the cells displayed EMT-like morphological alterations, including the loss of typical epithelial cobblestone morphology, acquisition of a fusiform mesenchymal shape and increased cell scattering and spindle-like polarization. Semiquantitative scoring illustrated that DAZAP1 protein was significantly upregulated in cancer compared with adjacent healthy gastric mucosa tissue (Fig. 1Eb).

The present study analyzed correlations between DAZAP1 expression and clinicopathological characteristics and prognosis in 90 GC tissue samples. High DAZAP1 expression was significantly associated with local invasion (T1/2 vs. T3/4), American Joint Committee on Cancer (AJCC) stage (I/II vs. III/IV), lymph node metastasis (N0 vs. N1) and tumor size (<5 vs. ≥5 cm). However, DAZAP1 was not linked to additional clinical characteristics, such as age, sex and differentiation in GC (Table SV). Kaplan-Meier survival analysis demonstrated a relationship between DAZAP1 levels and overall survival time (Fig. 1Fa). This correlation detected in individuals with late-stage GC (AJCC stage III/IV; Fig. 1Fc) was more noticeable than that in early-stage GC (AJCC stage I/II; Fig. 1Fb). DAZAP1 expression demonstrated predictive value for overall survival in early-(AJCC I/II) and late-stage (AJCC III/IV) GC patient subgroups. These data illustrated that DAZAP1 is upregulated and has an oncogenic function in GC.

DAZAP1 overexpression promotes the malignant biological behavior of GC. MKN-45 GC cell line with relatively low and AGS and MKN-74 cell lines with relatively elevated endogenous DAZAP1 levels were selected for transfection and functional experiments (Fig. 1C). Stable transfectants were constructed via DAZAP1-sense plasmids in MKN-45 cells (Fig. S2A) or DAZAP1 was suppressed using siRNAp in AGS and MKN-74 cells (Fig. S2B), as demonstrated via western blot analysis and qPCR. Subsequently, colony formation assays

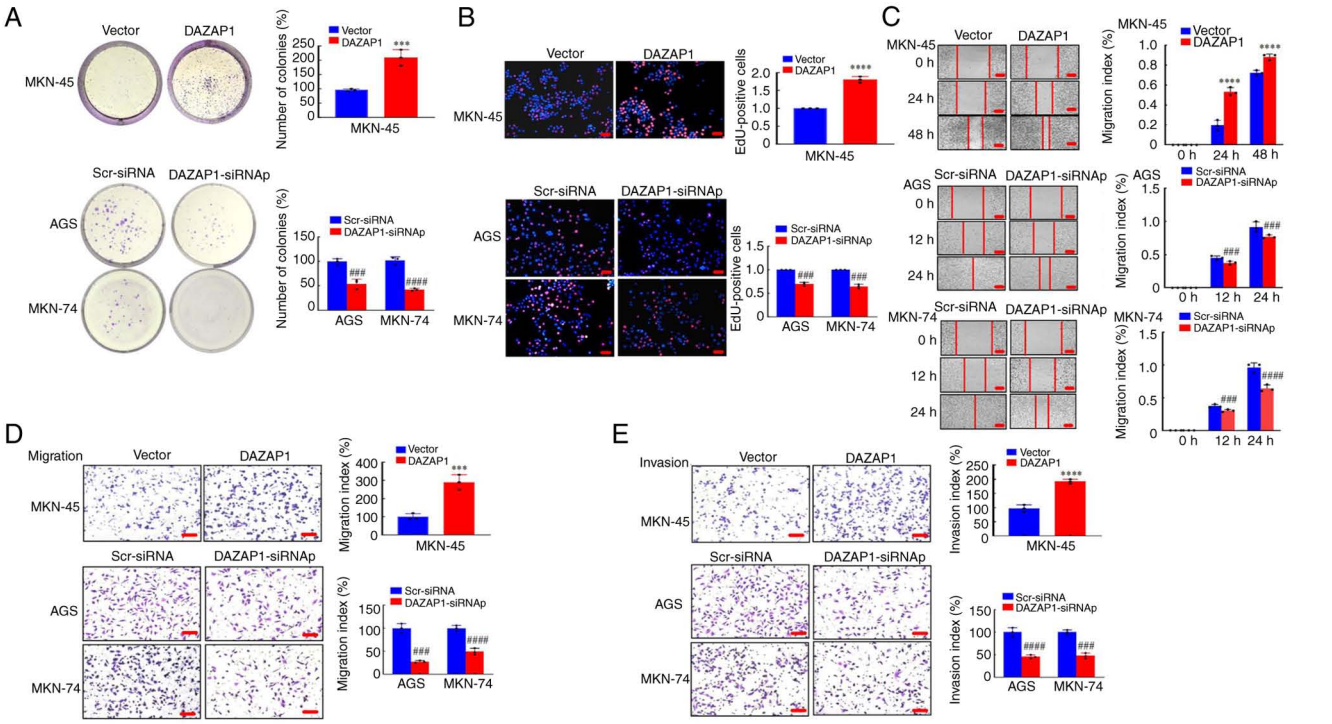

Figure 2. Functional analysis of DAZAP1 in GC cells *in vitro*. (A) Colony formation assay was performed to detect proliferative capability at 48 h. (B) EdU assay was used to determine the viability of GC cells. Red, EdU-positive cells; blue, Hoechst33258 (total cells). Scale bar, 100 μm. (C) Motility was determined wound healing assay. (D) Migration and (E) invasion assay were performed following transfection in GC cells. Scale bar, 150 μm. ***P<0.01, ****P<0.001 vs. vector; $^{###}$P<0.01, $^{####}$P<0.001 Scr-siRNA vs. DAZAP1-siRNAp. DAZAP1, deleted in azoospermia-associated protein 1; GC, gastric cancer; scr, scramble; si, small interfering; p, pool.

showed that overexpression of DAZAP1 led to significantly more colonies than the vector in MKN-45 cells (Fig. 2A). EdU assay showed that overexpression of DAZAP1 significantly induced cell proliferation compared with the control vector in MKN-45 cells (Fig. 2B). Proliferation of AGS and MKN-74 cells was inhibited by the knockdown of DAZAP1 (Fig. 2A and B).

The present study explored the effect of DAZAP1 on cell migration and invasion in GC. Wound healing assay demonstrated that the migration ability was promoted by DAZAP1 overexpression in MKN-45 cells, whereas DAZAP1 knockdown had the opposite effect on AGS and MKN-74 cells (Fig. 2C). Transwell experiments with or without Matrigel demonstrated a significant increase in migration and invasion following DAZAP1 overexpression and a significant decrease in migration and invasion in response to DAZAP1 knockdown (Fig. 2D). All these data illustrated that DAZAP1 mediated malignant phenotypes in GC cells *in vitro*.

DAZAP1 induces EMT in GC cells. A key step in tumor spreading is EMT, which occurs when epithelial cells associated with tumors transform into mesenchymal cells (27,28). The present study assessed cell morphology to see if DAZAP1 is essential for GC EMT. By contrast with the control cells, the MKN-45 cells that had DAZAP1 overexpression had an elongated spindle-like phenotype, which was distinguishable from normal mesenchymal cells (Fig. 3A).

Previous studies have shown that EMT improves motility and actin reorganization of cells (29,25). Therefore, F-actin was stained with phalloidin. In DAZAP1-overexpressing cells, F-actin filaments were more dispersed throughout the cytoplasm and localized at the protrusion rim compared with control cells (Fig. 3B). Immunofluorescence analysis revealed that DAZAP1 overexpression in MKN-45 cells downregulated E-cadherin and upregulated vimentin expression (Fig. 3C). Western blot analysis confirmed that DAZAP1 transfection altered the expression of EMT-associated markers. Overexpression of DAZAP1 significantly suppressed E-cadherin, whereas knockdown of DAZAP1 increased the expression of E-cadherin in GC cells (Fig. 3D). Conversely, overexpressing DAZAP1 promoted the expression of N-cadherin and vimentin, while knockdown of DAZAP1 suppressed their expression in GC cells (Fig. 3D).

Additionally, to explore the association between DAZAP1 and migration/invasion , the function of DAZAP1 in metastases was examined by injecting AGS/LV-pEGFP-DAZAP1-shRNA and AGS/LV-pEGFP-Scr-shRNA expressing GFP into nude mice (Fig. 3E). The knockdown efficiency of DAZAP1-shRNA was verified in AGS cells (Fig. S4C). Smaller lung metastatic nodules were detected in the LV-DAZAP1-shRNA compared with the LV-pEGFP-Scr-shRNA group (Fig. 3F). Histological examination confirmed the presence of GC cell metastases in the lung tissue (Fig. 3G). Moreover, IHC analysis demonstrated that vimentin protein levels were promoted in cancer tissue of the LV-pEGFP-Scr-shRNA compared with those in the LV-DAZAP1-shRNA group (Fig. 3H). These results indicated that DAZAP1 in GC cells may be a vital contributor to EMT progression, thereby mediating the ability of GC cells to migrate and invade.

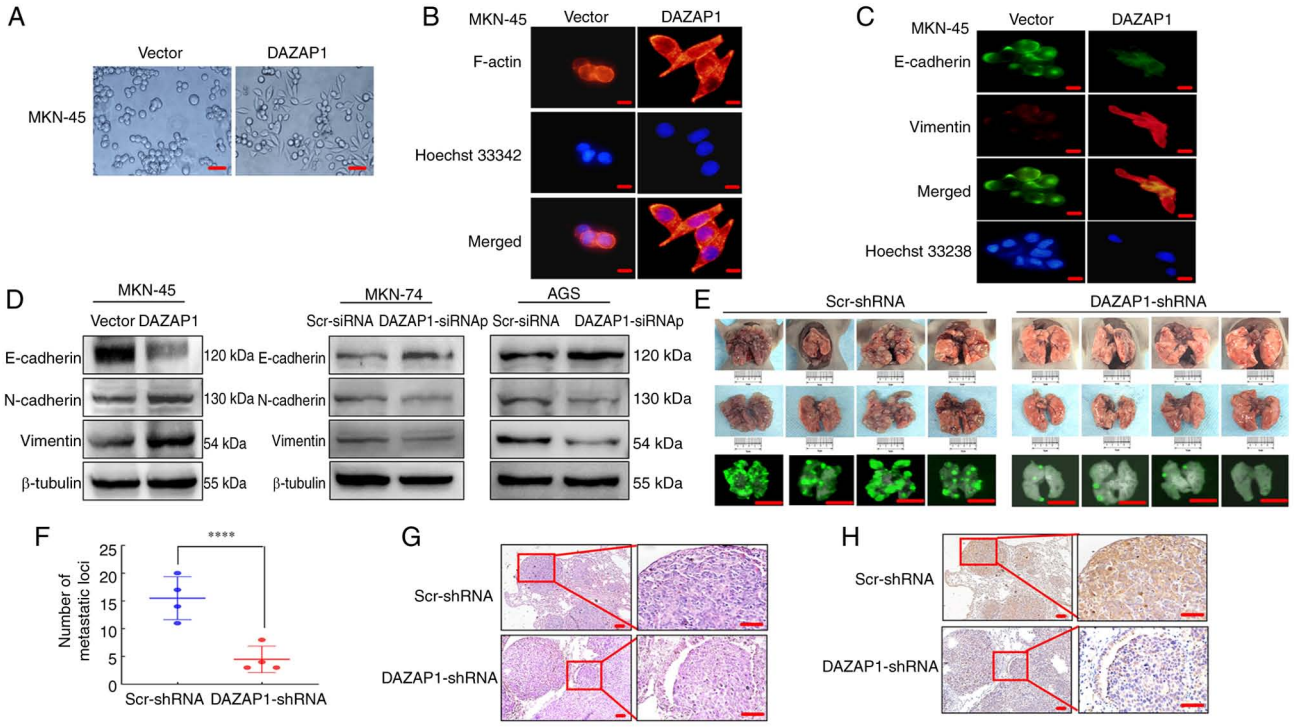

Figure 3. DAZAP1 induces EMT in GC cells. (A) Phase-contrast microscopy in MKN-45 cells. Scale bar, 50 μm. (B) F-actin expression and localization were analyzed by immunocytochemistry. The cytoskeleton and nuclei were stained with rhodamine-phallotoxin (red) and Hoechst33258 (blue). (C) Immunofluorescence staining for E-cadherin (green) and vimentin (red) in MKN-45 cells. Scale bar, 20 μm. (D) EMT biomarkers, including E-cadherin, N-cadherin and vimentin, were detected by western blotting in GC cells. (E) Representative metastatic tumors in the lungs from mice (n=4/group). Scale bar, 1 cm. (F) Number of metastatic tumors in the lung was counted. (G) Hematoxylin and eosin staining of lung sections of mice. (H) Immunohistochemical staining of vimentin. Scale bar, 100 μm. ****P<0.001. DAZAP, deleted in azoospermia-associated protein 1; EMT, epithelial-mesenchymal transition; GC, gastric cancer; scr, scramble; si, small interfering; sh, short hairpin.

DAZAP1 physically binds NOTCH1 or JAG1 mRNA to regulate its stability. As DAZAP1 is an RBP and regulates mRNAs by binding UAGKWWR motifs (9,11,12) (Fig. 4A), RIP-seq was performed in AGS cells to detect potential RNA targets. A total of 980 genes (1,376 transcripts) potentially bound to DAZAP1 (Table SVI). EMT-related genes were obtained from the EMT database (emtome.org) (Table SVII) (25,30).

The 980 DAZAP1-bound genes and the EMT-related genes from the database were used to construct a Venn diagram for identifying common genes (Fig. 4B). The intersection illustrated 88 genes (Table SVIII), among which 44 genes were associated with GC. These target genes were used for KEGG) pathway enrichment analyses. A total of 10 significantly enriched KEGG pathways, including 'pathways in cancer', were identified (Fig. 4C; Table SIX). NOTCH1 and JAG1 are essential in tumor progression and enriched in 'pathways in cancer' (16,18). Therefore, NOTCH1 and JAG1 were selected for subsequent study.

qPCR was performed to determine NOTCH1 and JAG1 mRNA expression in GC cells with DAZAP1 suppression; DAZAP1 knockdown group exhibited a significant decrease in NOTCH1 and JAG1 mRNA expression compared with the negative control group (Fig. 4D). RIP was performed to determine whether DAZAP1 binds to the NOTCH1 or JAG1 genes. Compared with IgG control, DAZAP1 antibody demonstrated notable enrichment of NOTCH1 and JAG1 RNA (Fig. 4E and F). The results demonstrated a physical association between the DAZAP1 protein and either NOTCH1 or JAG1 mRNA *in vitro*.

The present study explored the effect of DAZAP1 on NOTCH1 or JAG1 mRNA stability. Actinomycin D assay demonstrated that the half-life of NOTCH1 or JAG1 mRNA was significantly lower following DAZAP1 knockdown than in the control group in AGS cells (Fig. 4G and H). These data suggest that DAZAP1 can increase NOTCH1 or JAG1 expression by binding NOTCH1 or JAG1 mRNA and enhancing its stability.

DAZAP1 protein is composed of three primary domains: RRM1 (10-97 aa), RRM2 (113-190 aa) and CTD (250-407 aa). To investigate the domain required for DAZAP1-mediated NOTCH1 or JAG1 expression, DAZAP1 [full-length (FL)], including RRM-F1 (1-112 aa), RRM2-F2 (113-249 aa) and CTD-F3 (250-407 aa) plasmids with a FLAG-tag, were constructed (Fig. 4I). The *in vitro* binding assay showed that for NOTCH1 (Fig. 4J) and JAG1 (Fig. 4K) mRNA, the Flag group of full-length DAZAP1 (-FL) and its CTD domain (-F3) exhibited markedly high fold enrichment, while RRM1 (-F1) and RRM2 (-F2) only had weak enrichment. Thus, CTD is key for DAZAP1 to physically bind NOTCH1/JAG1 mRNA, thereby regulating their stability.

Overexpression of DAZAP1 promotes NOTCH1- or JAG1-mediated migration/invasion via EMT in GC cells. Ligands for NOTCH1 are transmembrane proteins expressed on adjacent cells, including JAG and Δ (14,15,23). The present

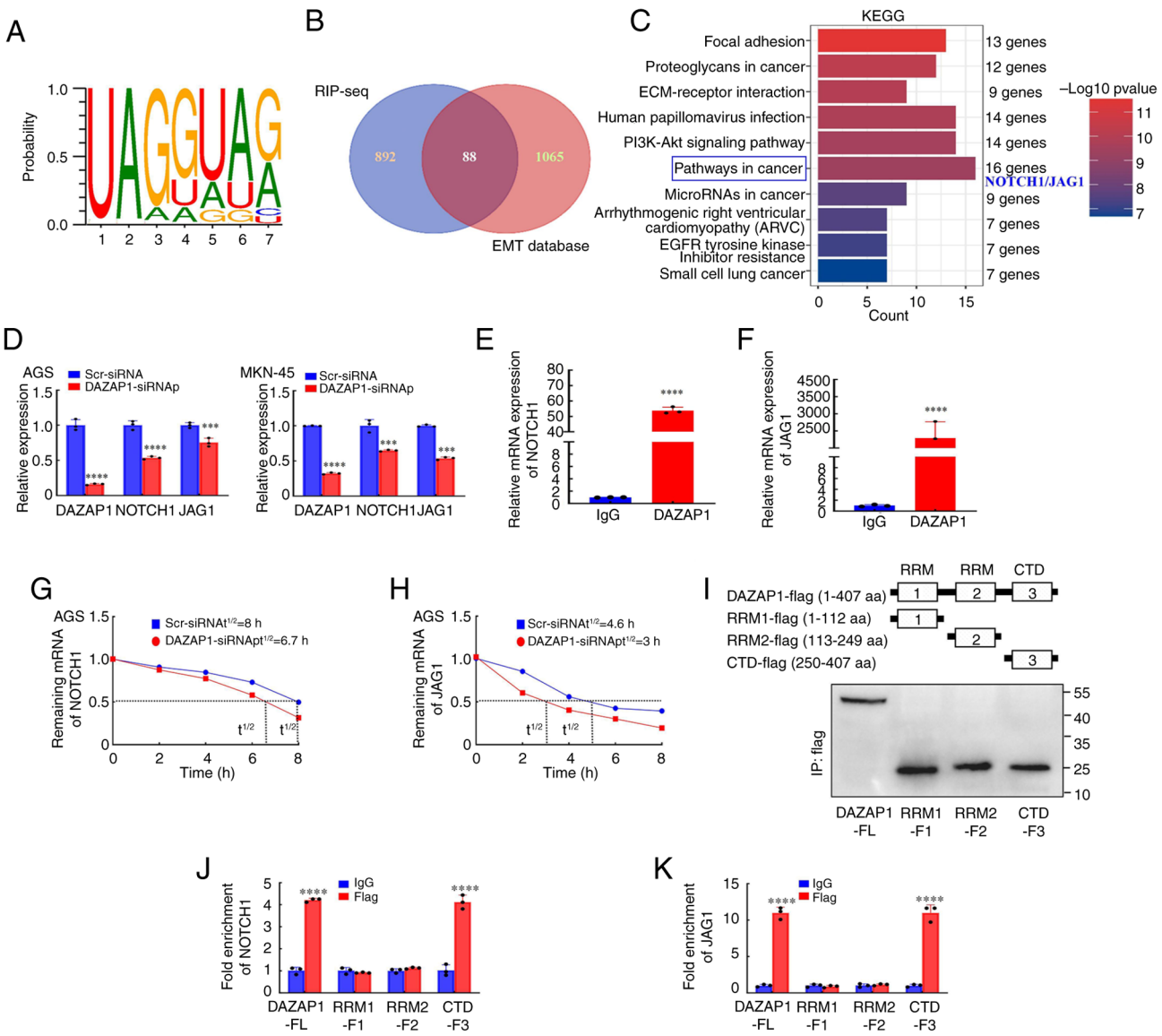

Figure 4. DAZAP1 binds NOTCH1 or JAG1 mRNA in GC cells. (A) DAZAP1-binding motif was predicted using the RBPmap database (rbpmap.technion.ac.il/). (B) Overlap between DAZAP1-interacting genes identified using RIP-seq and EMT-related genes from the EMT database (emtome.org). (C) Quantification of target genes involved in the pathways in the cancer signaling pathway, including NOTCH1 and JAG1, according to KEGG analysis in the WebGestalt database (webgestalt.org/). (D) RT-qPCR analysis of the mRNA levels of NOTCH1 and JAG1 following DAZAP1 knockdown in AGS and MKN-45 cells. RT-qPCR analysis of (E) NOTCH1 and (F) JAG1 with anti-DAZAP1 and IgG control antibodies in AGS cells. (G) NOTCH1 and (H) JAG1 mRNA $t_{1/2}$ in DAZAP1 knockdown AGS cells. n=3. (I) Verification of full-length or truncated DAZAP1 plasmids using western blotting and anti-FLAG antibody. RIP assay analysis of (J) NOTCH1 and (K) JAG1 mRNA binding to the DAZAP1 structure domains. ***P<0.01 and ****P<0.001 vs. scr-siRNA. RRM, RNA recognition motif; CTD, C-terminal domain; DAZAP1, deleted in azoospermia-associated protein 1; RIP-seq, RNA Immunoprecipitation-sequencing; EMT, Epithelial-Mesenchymal Transition; KEGG, Kyoto Encyclopedia of Genes and Genomes; RT-q, Reverse Transcription quantitative real-time; $t_{1/2}$, half-life; scr, scramble; si, small interfering; F, Fragment; FL, Full-Length; aa, amino acid.

study assessed whether DAZAP1/NOTCH1 or DAZAP1/JAG1 pathways contribute to GC cell progression. First, the present study constructed stable transfectants using NOTCH1- and JAG1-sense plasmids or knockdown of NOTCH1 and JAG1 with siRNAp in MKN-45 and AGS cells (Fig. S3A), as confirmed by western blot and RT-qPCR analysis. DAZAP1 knockdown attenuated the migratory and invasive abilities of GC cells, whereas overexpression of NOTCH1 or JAG1 partially reversed the phenotypes induced by DAZAP1 suppression compared with the control, as demonstrated by wound healing and Transwell assays (Figs. 5A-D and S4A-D). Rescue experiments showed that DAZAP1 overexpression markedly increased cell motility ability, which was abrogated by downregulation of NOTCH1 or JAG1 (Figs. 5A-D and S4A-D).

EMT-associated marker levels were detected by western blotting, indicating that DAZAP1 suppression elevated the expression of the epithelial marker (E-cadherin) and decreased expression of mesenchymal markers (vimentin and N-cadherin) in GC, Notably, this effect was reversed when NOTCH1 or JAG1 was introduced alongside DAZAP1 suppression (Figs. 5E and F and S4E-F). Conversely, DAZAP1 overexpression decreased E-cadherin expression and increased vimentin/N-cadherin levels in GC- and this trend was abolished when NOTCH1 or JAG1 expression was concurrently reduced. (Figs. 5E-F and S4E-F). These results indicated

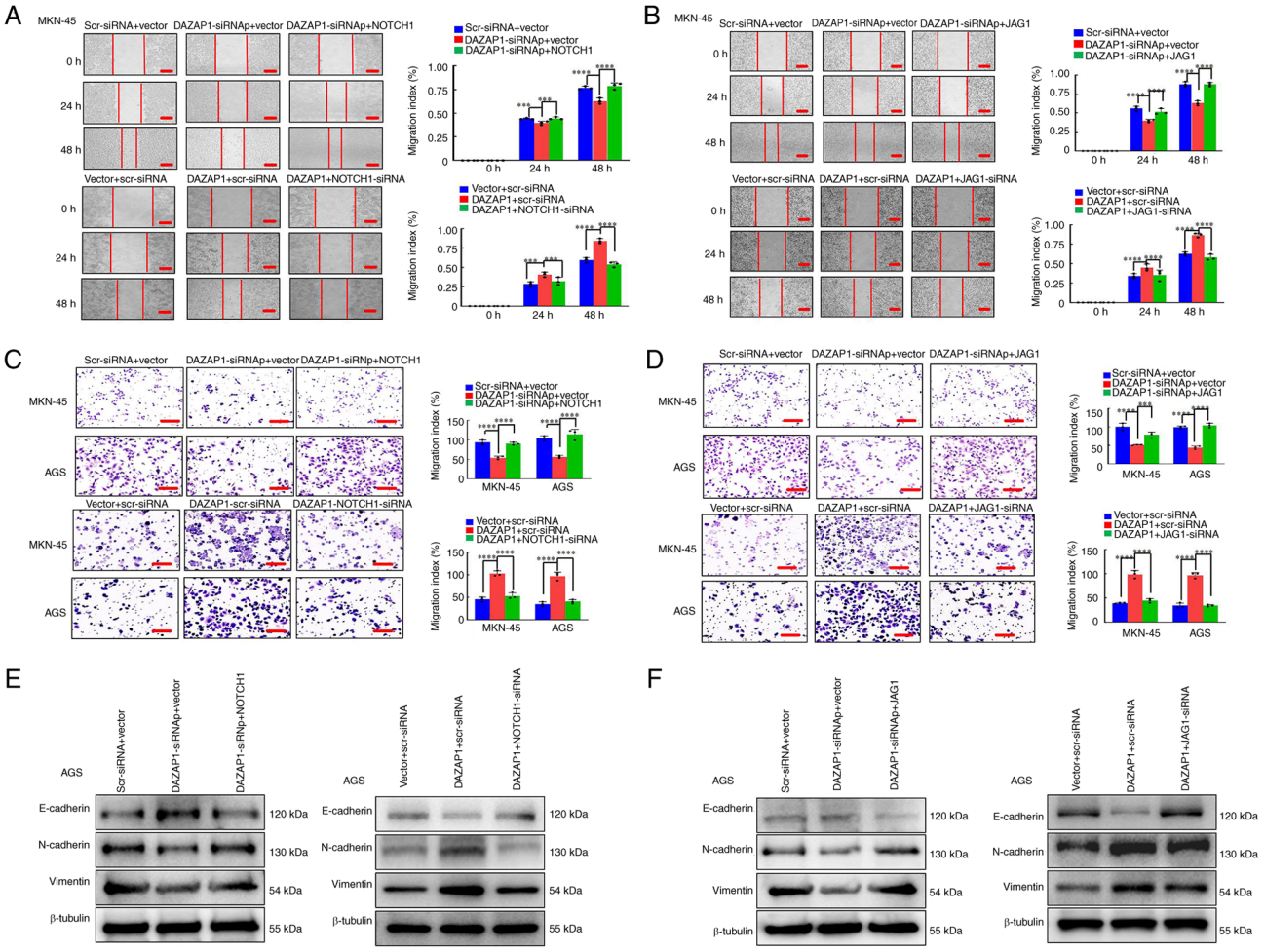

Figure 5. DAZAP1 regulates NOTCH1 or JAG1 expression to affect migration/invasion via epithelial-mesenchymal transition in GC cells. The wound healing assay in MKN-45 cells confirmed that DAZAP1 regulated (A) NOTCH1(A) and JAG1. (B) Scale bar, 100 μm. The Transwell migration assay confirmed that DAZAP1 regulates NOTCH1(C) and JAG1 (D) in MKN-45 and AGS cells, Scale bar, 150 μm. Expression of epithelial marker E-cadherin and mesenchymal markers vimentin and N-cadherin was detected by western blotting with β-tubulin as the internal control in AGS cells. The western blotting in AGS cells confirmed that DAZAP1 regulates NOTCH1 (E) and JAG1 (F). ***P<0.01, ****P<0.001. DAZAP1, deleted in azoospermia-associated protein 1; GC, gastric cancer; scr, scramble; si, small interfering.

that upregulation of DAZAP1 facilitated NOTCH1 or JAG1 expression to promote motility of GC cells via EMT.

Forced expression of DAZAP1 facilitates NOTCH1- and JAG1-mediated migration/invasion via EMT in GC cells. The present study examined whether NOTCH1 and JAG1 mediate the influence of DAZAP1 on GC cell migration and invasion. DAZAP1 overexpression vector increased motility capacity compared with the control, while DAZAP1/NOTCH1-siRNA suppressed migration/invasion capacity compared with DAZAP1 in GC cells (Figs. 6A-C and S5A and B). Reintroduction of JAG1 partially reversed the suppression compared with DAZAP1/NOTCH1-siRNA, as demonstrated by wound healing and Transwell assay (Figs. 6A-C and S5A and B).

Levels of epithelial marker E-cadherin were downregulated in DAZAP1 compared with control, while DAZAP1/NOTCH1-siRNAed result in upregulated E-cadherin compared with DAZAP1. However, E-cadherin upregulation was partly reversed following DAZAP1/NOTCH1-siRNA/JAG1 transfection. Mesenchymal markers vimentin and N-cadherin were upregulated in the DAZAP1 overexpression group relative to the vector, downregulated in the DAZAP1/NOTCH1-siRNA group compared with the DAZAP1 overexpression group and partially restored following DAZAP1/NOTCH1-siRNA/JAG1 transfection (Fig. 6D).

To investigate the effect of DAZAP1-NOTCH1-JAG1 on cell metastasis *in vivo*, the AGS cells expressing the LV-vector, LV-DAZAP1, DAZAP1/NOTCH1-shRNA or DAZAP1/NOTCH1-shRNA/JAG1 were implanted into the tail vein of nude mice, thereby causing lung metastases (Fig. 6E). The knockdown efficiency of NOTCH1-shRNA was verified in AGS cells (Fig. S3C). More metastatic tumors were determined in DAZAP1 overexpression compared with the vector group; DAZAP1/NOTCH1-shRNA caused a significant decrease in the number of visible tumors than in the control (Fig. 6F). However, the reintroduction of JAG1 partially reversed the suppression compared with DAZAP1/NOTCH1-shRNA, which was associated with an increased count of metastasis loci (Fig. 6F). The GC metastases in the lung of nude mice were confirmed through

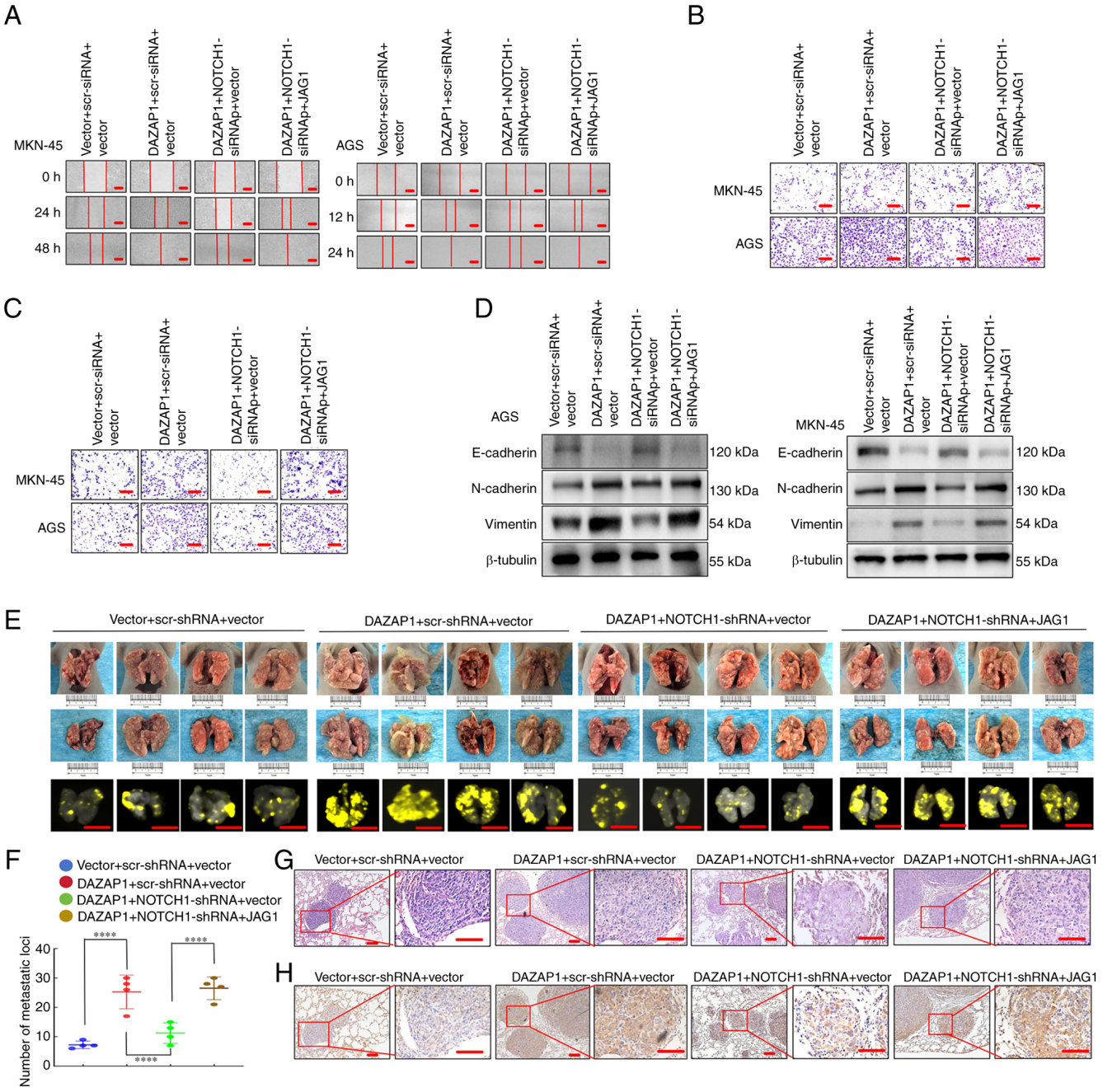

Figure 6. DAZAP1 promotes NOTCH1 and JAG1 expression to alter migration/invasion via epithelial-mesenchymal transition in gastric cancer cells. (A) Cell migration was tested using a monolayer wound healing assay. Scale bar, 100 μm. (B) Migration and (C) invasion assay. Scale bar, 150 μm. (D) Epithelial (E-cadherin) and mesenchymal markers (N-cadherin, vimentin) were detected by western blotting in AGS and MKN-45 cells. (E) Lung samples were collected from mice injected with AGS cells via the tail vein. Scale bar, 1 cm (F) Lung metastatic nodules were counted. (G) Hematoxylin and eosin and (H) vimentin staining were conducted on lung samples from these mice. Scale bar, 100 μm. ****P<0.001. DAZAP1, deleted in azoospermia-associated protein 1; scr, scramble; si, small interfering; sh, short hairpin.

hematoxylin and eosin staining (Fig. 6G), and the difference in cell motility was detected by vimentin IHC staining. Vimentin is a well-characterized mesenchymal marker that is associated with cancer cell migratory and invasive potential as well as metastatic ability (31-32). Vimentin was upregulated in the DAZAP1 overexpression group relative to the vector, downregulated in the DAZAP1/NOTCH1-siRNA group compared with the DAZAP1 overexpression group and partially restored following DAZAP1/NOTCH1-siRNA/JAG1 transfection (Fig. 6H). Therefore, DAZAP1 modulated NOTCH1/JAG1 signaling in GC cells to promote invasion and metastasis.

DAZAP1 expression is positively associated to NOTCH1 or JAG1 expression in GC. The present study assessed the expression of DAZAP1, NOTCH1 and JAG1 in 10 freshly collected GC biopsy samples. Western blotting (Fig. 7A) and RT-qPCR (Fig. 7B and C) demonstrated that the expression of DAZAP1, NOTCH1 and JAG1 was significantly upregulated compared with adjacent normal tissue. DAZAP1 expression

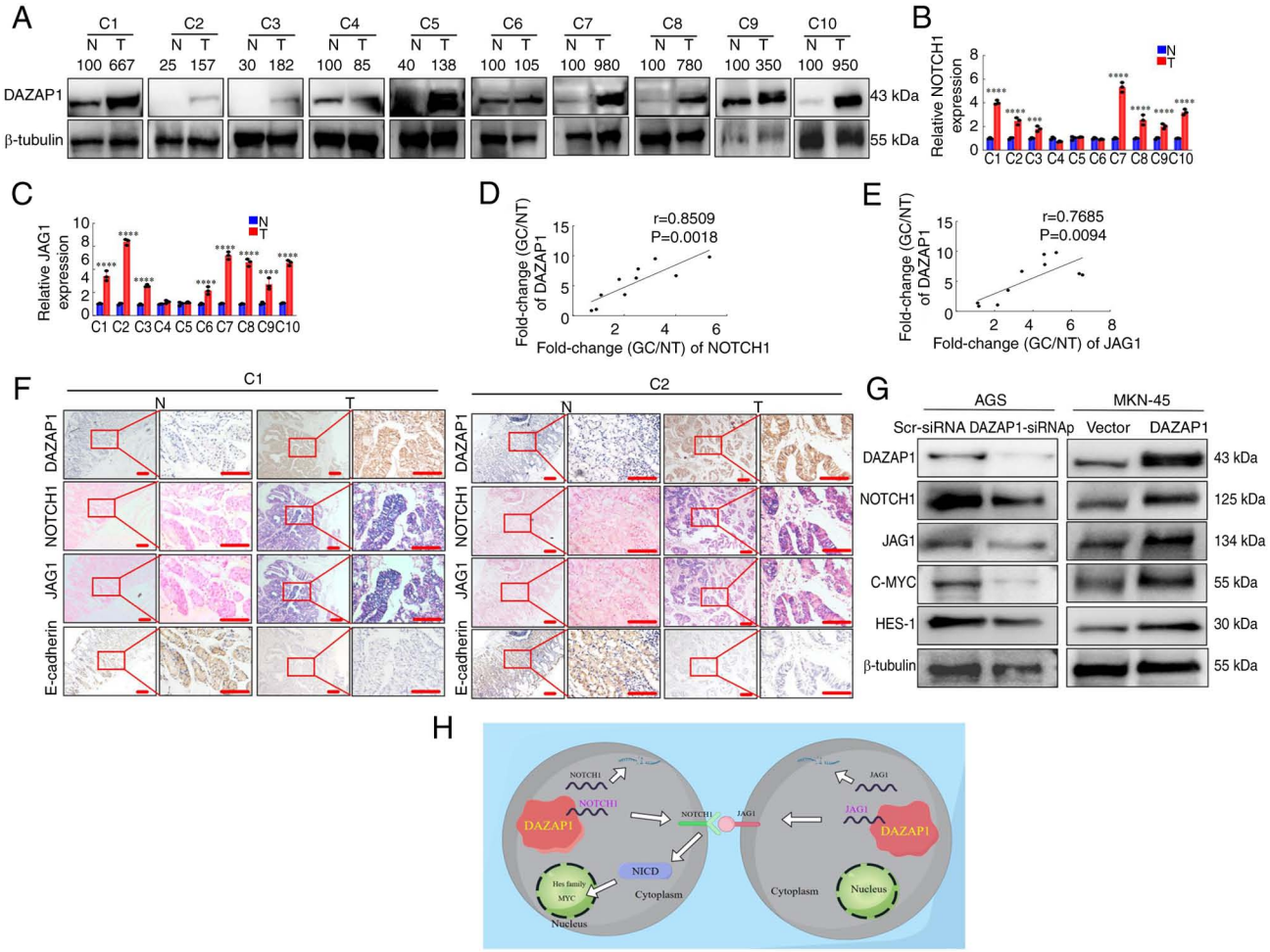

Figure 7. DAZAP1 expression is positively correlated with NOTCH1 or JAG1 mRNA expression in GC tissues. (A) Expression of DAZAP1 and (B) Expression levels of NOTCH1 in 10 paired N and GC tissue specimens were detected by qPCR. ***P<0.01, ****P<0.001 (C) Expression levels of JAG1 in 10 paired N and GC tissue specimens were detected by qPCR. ****P<0.001 (D) Correlation between DAZAP1 and (D) NOTCH1 in 10 GC tissue samples. (E) Correlation between DAZAP1 and JAG1 in 10 GC tissue samples. (F) Gene expression in N and GC tissue was evaluated using immunohistochemistry and *in situ* hybridization. (G) Abnormal expression of DAZAP1 modulated the NOTCH1 signaling pathway, as detected by western blot analysis. (H) Signal transduction mechanism of DAZAP1. Scale bar, 100 μm. DAZAP1, deleted in azoospermia-associated protein 1; GC, gastric cancer; N, normal; T, tumor; HES, Hairy and Enhancer of Split 1; NICD, Notch intracellular domain; C, case; scr, scramble; si, small interfering.

was positively associated with NOTCH1 or JAG1 expression (Fig. 7D and E).

IHC and ISH were demonstrated that the expression of DAZAP1, NOTCH1 and JAG1 was significantly higher, while that of E-cadherin was significantly lower, in GC compared with healthy tissue (Fig. 7F).

Aberrant NOTCH signaling activation is typically linked to its receptors and ligands (33-35). To determine whether DAZAP1 impacts the NOTCH1 signaling pathway, the present study examined the expression of key components in the NOTCH1 pathway using western blot analysis in GC cells. Knockdown of DAZAP1 decreased NOTCH1, JAG1, MYC and hairy and enhancer of split homolog-1 (HES-1) protein expression in AGS cells. Conversely, forced expression of DAZAP1 resulted in increased NOTCH1, JAG1, MYC and HES-1 levels in MKN-45 cells.

Collectively, these data demonstrated that DAZAP1 expression was positively associated with levels of NOTCH1 and JAG1 in GC samples and DAZAP1 facilitated the activation of the NOTCH1 signaling pathway.

For the potential transcription factors of DAZAP1, predictions were made using the AnimalTFDB v4.0 database, which identified a total of 796 putative transcription factors (Table SX).

Discussion

Numerous investigations have concluded that several molecular mechanisms participate in the genesis, prognostication and treatment options in GC (2,7,16,28). However, GC progression remains uninvestigated. The present study identified a novel target, DAZAP1, in GC cell progression via the EMT process, which could promote NOTCH1 and JAG1 mRNA expression and mediate the stimulation of the NOTCH1 pathway. Hence, the DAZAP1-NOTCH1-JAG1 axis may participate in GC progression (Fig. 7H).

DAZAP1 gene is positioned on the short arm of human chromosome 19, region 19p13, and is part of a subfamily of hnRNP genes (8,9). Its abnormal expression is associated with certain types of cancers. For example, DAZAP1 is

upregulated in hepatic carcinoma, which indicates a poor prognosis (36). Moreover, DAZAP1 is significantly upregulated in pancreatic cancer (PC) tissue and cell lines compared with normal counterparts (37). DAZAP1 suppression inhibits PC cell proliferation and triggers ferroptosis, while inhibiting ferroptosis reverses these impacts, promoting PC cell proliferation and migration/invasion (37). Nevertheless, the role of DAZAP1 in GC is unknown. Here, high DAZAP1 expression was significantly associated with poor prognosis in patients with GC. Furthermore, DAZAP1 overexpression markedly enhanced GC cell motility and invasion, whereas DAZAP1 knockdown markedly decreased these. Upregulation of DAZAP1 increased the levels of the EMT-associated genes N-cadherin and vimentin and decreased E-cadherin levels. Previous reports have shown that heterogeneous nuclear ribonucleoprotein F, part of the hnRNP family, regulates EMT in bladder cancer (38,39), which agrees with the present data. These outcomes illustrated that DAZAP1 has an oncogenic function and triggers GC onset and progression.

DAZAP1 is a multifunctional RBP (10,12,13). For example, DAZAP1 enhances cytochrome c oxidase 16 expression by regulating pre-mRNA alternative splicing, thereby promoting OSCC invasion and mitochondrial respiration (10). DAZAP1 triggers tumor progression in GC stem cells and modulates the splicing and expression of the mitophagy-associated gene unc-51 like autophagy activating kinase 1 (40). The present study searched for putative gene targets of DAZAP1 and demonstrated that DAZAP1 physically associated with NOTCH1 or JAG1 mRNA to enhance NOTCH1 or JAG1 mRNA stability. Moreover, the specific binding domains of DAZAP1 in NOTCH1 or JAG1 were confirmed. Among the NOTCH receptors, NOTCH1 has been extensively investigated and identified in tumor tissue more often than any other member (16,23,35,36). Previous studies have demonstrated elevated expression of NOTCH1 in GC tissue are associated with tumor migration/invasion, depth of invasion and vessel invasion (16,41). JAG1 is a canonical ligand for Notch receptors, and its upregulation has been observed in numerous types of cancer, such as GC and breast cancer (BC), where it facilitates proliferation and migration/invasion (18,20,21) Formerly, reports have shown that RBP ZFP36 family members ZFP36L1 and ZFP36L2 suppress NOTCH1 expression via interaction with sequences in the NOTCH1 3' untranslated region (UTR) to modulate tumor development and progression (42,43). ZFP36 binds the 3' UTR of JAG1 and post-transcriptionally suppresses JAG1 expression, leading to decreased JAG1 protein levels and impaired angiogenic sprouting (21), which were consistent with the present findings. In addition, wound healing and Transwell assays revealed that DAZAP1 increased GC cell motility, while DAZAP1 knockdown abrogated the facilitation of GC cell invasion and migration mediated by NOTCH1 or JAG1 knockdown, thereby regulating the EMT process in GC cells. Thus, the present data indicated that DAZAP1 was a common binding partner of NOTCH1 or JAG1 and associated with migration and invasion in GC cells.

NOTCH pathways are typically regarded as ligand-induced (44,45), and the receptors and ligands are highly co-expressed in malignancy (45,46). NOTCH ligand JAG1 is hypothesized to enhance the metastatic potential of tumor cells via NOTCH-dependent induction of EMT (23,47). NOTCH suppression prevents JAG1-mediated NOTCH signaling from promoting EMT, migration and invasion of BC cells (23). Nevertheless, the mechanism by which NOTCH1 and JAG1 are regulated by DAZAP1 to promote GC cell invasiveness needs further investigation. Here, overexpression of DAZAP1 caused an increase in migration/invasion capacity compared with vector, while DAZAP1 + NOTCH1-siRNAp suppressed motility compared with DAZAP1 in GC cells. Yet, the reintroduction of JAG1 partially reversed the suppression compared with DAZAP1 + NOTCH1-siRNAp in GC cells. Western blotting demonstrated upregulation of these molecules decreased epithelial marker E-cadherin, with concomitant increased mesenchymal marker vimentin and N-cadherin expression in GC cells. Hence, it was hypothesized that DAZAP, NOTCH1 and JAG1 coregulated GC cell expression and motility via the EMT process.

However, the present study had limitations. Firstly, the present study did not identify the potential transcription factors of DAZAP1. Future studies should investigate the transcription factors and other regulatory mechanisms of DAZAP1. Secondly, the present study was primarily conducted in cell lines and animal models, and further validation is required in larger cohorts of clinical GC samples to confirm the clinical relevance of the present findings.

In conclusion, DAZAP1 expression was significantly increased in GC tissue and may be an indicator of poor prognosis for patients. In addition to mediating the stability of NOTCH1 and/or JAG1 mRNA, which regulates EMT, DAZAP1 is key for GC cell invasion and metastatic promotion. Therefore, the aforementioned molecules provide not only a predictor for GC prognosis but also a potential therapeutic target.

Acknowledgements

Not applicable.

Funding

The present study was supported by the National Natural Science Foundation of China (grant nos. 82273354, 82372955, 82073066, 82302891 and 82403543), Guangdong Basic and Applied Basic Research Foundation (grant no. 2024A1515012891), Science and Technology Program of Guangzhou (grant nos. 2024A04J5133 and (2025A04J3637) and the Science and Technology Planning Project of Guangdong Province (grant no. 2017B030314037).

Availability of data and materials

The data generated in the present study may be found in the National Center for Biotechnology Information database under accession no SRX31515429. or at the following URL: ncbi.nlm.nih.gov/sra/PRJNA1378511.

Authors' contributions

JDW, JW, YFH, AML and SDL and JX conceived and designed the study. SYP, YDC, JKW, XDH, LJH, YCX, TYL, XYW, PY and JMZ performed experiments. QY and GNL collected tissue samples and analyzed and interpreted data. JYL and

WYD analyzed data. YFH, AML and SDL supervised the study. SYP and JDW wrote the manuscript and confirm the authenticity of all the raw data. All authors have read and approved the final manuscript.

Ethics approval and consent to participate

The animal experimental protocols were approved by the Animal Ethics Committee of Nanfang Hospital, Southern Medical University, Guangzhou, China (approval no. IACUC-LAC-20250111-002). The use of tissue chips was approved by the Ethics Committee of Shanghai Outdo Biotech Co. Ltd, Shanghai, China (approval no. SHYJS-CP-1804015). Additionally, the research involving human tissue received ethical approval from the Ethics Committee of Nanfang Hospital, Guangzhou, China (approval no. NFEC-202105-K18). Written informed consent was obtained from all participants.

Patient consent for publication

Not applicable.

Competing interests

The authors declare that they have no competing interests.

References

1. Ferlay J, Colombet M, Soerjomataram I, Parkin DM, Piñeros M, Znaor A and Bray F: Cancer statistics for the year 2020: An overview. Int J Cancer: April 5, 2021 (Epub ahead of print).
2. Wang SY, Yang XQ, Wang YX, Shen A, Liang CC, Huang RJ, Cheng UH, Jian R, An N, Xiao YL, *et al*: Overexpression of COX7A1 promotes the resistance of gastric cancer to oxaliplatin and weakens the efficacy of immunotherapy. Lab Invest 104: 102090, 2024.
3. Chen Z, Chen Y, Sun Y, Tang L, Zhang L, Hu Y, He M, Li Z, Cheng S, Yuan J, *et al*: Predicting gastric cancer response to anti-HER2 therapy or anti-HER2 combined immunotherapy based on multi-modal data. Signal Transduct Target Ther 9: 222, 2024.
4. Chen LY, Wang LW, Wen J, Cao JD, Zhou R, Yang JL, Xiao Y, Su T, Huang Y, Guo Q, *et al*: RNA-binding protein YBX3 promotes pparγ-SLC3A2 mediated BCAA metabolism fueling brown adipogenesis and thermogenesis. Mol Metab 90: 102053, 2024.
5. He S, Valkov E, Cheloufi S and Murn J: The nexus between RNA-binding proteins and their effectors. Nat Rev Genet 24: 276-294, 2023.
6. Podszywalow-Bartnicka P and Neugebauer KM: Multiple roles for AU-rich RNA binding proteins in the development of haematologic malignancies and their resistance to chemotherapy. RNA Biol 21: 1-17, 2024.
7. Li J, Pei M, Xiao W, Liu X, Hong L, Yu Z, Peng Y, Zhang J, Yang P, Lin J, *et al*: The HOXD9-mediated PAXIP1-AS1 regulates gastric cancer progression through PABPC1/PAK1 modulation. Cell Death Dis 14: 341, 2023.
8. Choudhury R, Roy SG, Tsai YS, Tripathy A, Graves LM and Wang Z: The splicing activator DAZAP1 integrates splicing control into MEK/Erk-regulated cell proliferation and migration. Nat Commun 5: 3078, 2014.
9. Yang HT, Peggie M, Cohen P and Rousseau S: DAZAP1 interacts via its RNA-recognition motifs with the C-termini of other RNA-binding proteins. Biochem Biophys Res Commun 380: 705-709, 2009.
10. Zhang J, Ni Z, Zhang Y, Guo Y, Zhai R, Wang M, Gong Z, Wang M, Zeng F, Gu Z, *et al*: Dazap1 phase separation regulates mitochondrial metabolism to facilitate invasion and metastasis of oral squamous cell carcinoma. Cancer Res 84: 3818-3833, 2024.
11. Sasaki K, Ono M, Takabe K, Suzuki A and Kurihara Y: Specific intron-dependent loading of DAZAP1 onto the cox6c transcript suppresses pre-mrna splicing efficacy and induces cell growth retardation. Gene 657: 1-8, 2018.
12. Wang Q, Guo Y, Wang W, Liu B, Yang G, Xu Z, Li J and Liu Z: RNA binding protein DAZAP1 promotes HCC progression and regulates ferroptosis by interacting with SLC7A11 mRNA. Exp Cell Res 399: 112453, 2021.
13. Zhou Y, Huangfu S, Li M, Tang C, Qian J, Guo M, Zhou Z, Yang Y and Gu C: DAZAP1 facilitates the alternative splicing of KITLG to promote multiple myeloma cell proliferation via ERK signaling pathway. Aging 14: 7972-7685, 2022.
14. Platonova N, Lesma E, Basile A, Bignotto M, Garavelli S, Palano MT, Moschini A, Neri A, Colombo M and Chiaramonte R: Targeting notch as a therapeutic approach for human malignancies. Curr Pharm Des 23: 108-134, 2017.
15. Yeh TS, Wu CW, Hsu KW, Liao WJ, Yang MC, Li AF, Wang AM, Kuo ML and Chi CW: The activated Notch1 signal pathway is associated with gastric cancer progression through cyclooxygenase-2. Cancer Res 69: 5039-5048, 2009.
16. Ma H, Li N and Mo Z: Elevated Notch-1 expression promotes the lymph node metastasis of gastric cancer and the Notch-1-PTEN-ERK1/2 signalling axis promotes the progression of gastric cancer. Cytokine 159: 156013, 2022.
17. Feng P, Chen D, Wang X, Li Y, Li Z, Li B, Zhang Y, Li W, Zhang J, Ye J, *et al*: Inhibition of the m(6)A reader IGF2BP2 as a strategy against T-cell acute lymphoblastic leukemia. Leukemia 36: 2180-2188, 2022.
18. Guo J, Zhang CD, An JX, Xiao YY, Shao S, Zhou NM and Dai DQ: Expression of miR-634 in gastric carcinoma and its effects on proliferation, migration, and invasion of gastric cancer cells. Cancer Med 7: 776-787, 2018.
19. Sugiyama M, Oki E, Nakaji Y, Tsutsumi S, Ono N, Nakanishi R, Sugiyama M, Nakashima Y, Sonoda H, Ohgaki K, *et al*: High expression of the Notch ligand Jagged-1 is associated with poor prognosis after surgery for colorectal cancer. Cancer Sci 107: 1705-1716, 2016.
20. Qiao X, Ma B, Sun W, Zhang N, Liu Y, Jia L and Liu C: JAG1 is associated with the prognosis and metastasis in breast cancer. Sci Rep 12: 21986, 2022.
21. Sunshine HL, Cicchetto AC, Kaczor-Urbanowicz KE, Ma F, Pi D, Symons C, Turner M, Shukla V, Christofk HR, Vallim TA and Iruela-Arispe ML: Endothelial Jagged1 levels and distribution are post-transcriptionally controlled by ZFP36 decay proteins. Cell Rep 43: 113627, 2024.
22. Gao Y, Cheng X and Han M: ZEB1-activated Notch1 promotes circulating tumor cell migration and invasion in lung squamous cell carcinoma. Clin Transl Oncol 25: 817-829, 2023.
23. Shao S, Zhao X, Zhang X, Luo M, Zuo X, Huang S, Wang Y, Gu S and Zhao X: Notch1 signaling regulates the epithelial-mesenchymal transition and invasion of breast cancer in a Slug-dependent manner. Mol Cancer 1: 28, 2015.
24. Paz I, Kosti I, Ares M Jr, Cline M and Mandel-Gutfreund Y: Rbpmap: A web server for mapping binding sites of RNA-binding proteins. Nucleic Acids Res 42: W361-W367, 2014.
25. Vasaikar SV, Deshmukh AP, den Hollander P, Addanki S, Kuburich NA, Kudaravalli S, Joseph R, Chang JT, Soundararajan R and Mani SA: Emtome: A resource for pan-cancer analysis of epithelial-mesenchymal transition genes and signatures. Br J Cancer 124: 259-269, 2021.
26. Livak KJ and Schmittgen TD: Analysis of relative gene expression data using real-time quantitative PCR and the 2(-Delta Delta C(T)) method. Methods 25: 402-408, 2001.
27. Xie R, Wang J, Tang W, Li Y, Peng Y, Zhang H, Liu G, Huang X, Zhao J, Li A, *et al*: Rufy3 promotes metastasis through epithelial-mesenchymal transition in colorectal cancer. Cancer Lett 390: 30-38, 2017.
28. Peng Y, Zhang P, Huang X, Yan Q, Wu M, Xie R, Wu Y, Zhang M, Nan Q, Zhao J, *et al*: Direct regulation of FOXK1 by C-jun promotes proliferation, invasion and metastasis in gastric cancer cells. Cell Death Dis 7: e2480, 2016.
29. Zhang P, Tang WM, Zhang H, Li YQ, Peng Y, Wang J, Liu GN, Huang XT, Zhao JJ, Li G, *et al*: MiR-646 inhibited cell proliferation and EMT-induced metastasis by targeting FOXK1 in gastric cancer. Br J Cancer 117: 525-534, 2017.
30. Liu H, Li Z, Zhang L, Zhang M, Liu S, Wang J, Yang C, Peng Q, Du C and Jiang N: Necroptosis-related prognostic model for pancreatic carcinoma reveals its invasion and metastasis potential through hybrid EMT and immune escape. Biomedicines 11: 1738, 2023.
31. Coelho-Rato LS, Parvanian S, Modi MK and Eriksson JE: Vimentin at the core of wound healing. Trends Cell Biol 34: 239-254, 2024.

32. Ridge KM, Eriksson JE, Pekny M and Goldman RD: Roles of vimentin in health and disease. Genes Dev 36: 391-407, 2022.
33. Goenka A, Khan F, Verma B, Sinha P, Dmello CC, Jogalekar MP, Gangadaran P and Ahn BC: Tumor microenvironment signaling and therapeutics in cancer progression. Cancer Commun (London) 43: 525-561, 2023.
34. Teoh SL and Das S: Notch signalling pathways and their importance in the treatment of cancers. Curr Drug Targets 19: 128-143, 2018.
35. Hassan WA and Ito T: Identifying specific Notch1 target proteins in lung carcinoma cells. Histol Histopathol 36: 69-76, 2021.
36. Deng JJ, Li GP, Lu W, Yan Z and Wang Y: DAZAP1 overexpression promotes growth of HCC cell lines: A primary study using CEUS. Clin Transl Oncol 24: 1168-1176, 2022.
37. Wang X, Fan H, Ye X, Hu Y, Xiao Y, Zhang M, Xu Y, Song J and Luo Y: RNA-binding protein DAZAP1 accelerates the advancement of pancreatic cancer by inhibiting ferroptosis. Eur J Med Res 30: 3, 2025.
38. Li F, Zhao H, Su M, Xie W, Fang Y, Du Y, Yu Z, Hou L and Tan W: HnRNP-F regulates EMT in bladder cancer by mediating the stabilization of Snail1 mRNA by binding to its 3' UTR. EBioMedicine 45: 208-219, 2019.
39. Li F, Xie W, Fang Y, Xie K, Liu W, Hou L and Tan W: HnRNP-F promotes the proliferation of bladder cancer cells mediated by PI3K/AKT/FOXO1. J Cancer 12: 281-291, 2021.
40. Zhang P, Wang W, Xiang H, Zhou Y, Peng Q, Liu G, Xu ZX and Lu L: DAZAP1 maintains gastric cancer stemness by inducing mitophagy. JCI Insight 10: e175422, 2025.
41. Zhou L, Yang Y, Ye Y, Qiao Q, Mi Y, Liu H, Zheng Y, Wang Y, Liu M and Zhou Y. Notch1 signaling pathway promotes growth and metastasis of gastric cancer via modulating CDH5. Aging 16: 11893-11903, 2024.
42. Hodson DJ, Janas ML, Galloway A, Bell SE, Andrews S, Li CM, Pannell R, Siebel CW, MacDonald HR, De Keersmaecker K, *et al*: Deletion of the RNA-binding proteins ZFP36L1 and ZFP36L2 leads to perturbed thymic development and T lymphoblastic leukemia. Nat Immunol 11: 717-724, 2010.
43. Petkau G, Mitchell TJ, Chakraborty K, Bell SE, D Angeli V, Matheson L, Turner DJ, Saveliev A, Gizlenci O, Salerno F, *et al*: The timing of differentiation and potency of CD8 effector function is set by RNA binding proteins. Nat Commun 13: 2274, 2022.
44. Shi Q, Xue C, Zeng Y, Yuan X, Chu Q, Jiang S, Wang J, Zhang Y, Zhu D and Li L: Notch signaling pathway in cancer: From mechanistic insights to targeted therapies. Signal Transduct Target Ther 9: 128, 2024.
45. Wang L, Cao G, Li W, Chen XW, Xiong SS, Mu YN, Jiang JF, Yang L, Zhang DR and Cao YW: Expressions and prognostic values of notch3 and DLL4 in human breast cancer. Technol Cancer Res Treat 22: 15330338221118984, 2023.
46. Zhao B, Hu S, Xiao Q, Fan S, Yu X, Li C, Dong P and Zheng J: Expression of NOTCH receptors and ligands and prognosis of hepatocellular carcinoma. Biomark Med 14: 1631-1639, 2020.
47. Su H, Wang X, Song J, Wang Y, Zhao Y and Meng J: Microrna-539 inhibits the progression of Wilms' Tumor through downregulation of JAG1 and Notch1/3. Cancer Biomark 24: 125-133, 2019.